J. Fluid Mech. (2014), *vol.* 757, *pp.* 550–572.
doi:10.1017/jfm.2014.515

Intermittency in the relative separations of tracers and of heavy particles in turbulent flows

L. Biferale[1,†], A. S. Lanotte[2], R. Scatamacchia[1,3] and F. Toschi[3,4,5]

[1]Department of Physics and INFN, University of Tor Vergata, Via della Ricerca Scientifica 1, 00133 Rome, Italy

[2]CNR-ISAC and INFN-Sez. Lecce, Str. Prov. Lecce-Monteroni, 73100 Lecce, Italy

[3]Department of Physics, Eindhoven University of Technology, 5600 MB Eindhoven, The Netherlands

[4]Department of Mathematics and Computer Science, Eindhoven University of Technology, 5600 MB Eindhoven, The Netherlands

[5]CNR-IAC, Via dei Taurini 19, 00185 Rome, Italy

(Received 2 March 2014; revised 4 August 2014; accepted 2 September 2014; first published online 23 September 2014)

Results from direct numerical simulations (DNS) of particle relative dispersion in three-dimensional homogeneous and isotropic turbulence at Reynolds number $Re_\lambda \sim 300$ are presented. We study point-like passive tracers and heavy particles, at Stokes number $St = 0.6$, 1 and 5. Particles are emitted from localised sources, in bunches of thousands, periodically in time, allowing an unprecedented statistical accuracy to be reached, with a total number of events for two-point observables of the order of 10^{11}. The right tail of the probability density function (PDF) for tracers develops a clear deviation from Richardson's self-similar prediction, pointing to the intermittent nature of the dispersion process. In our numerical experiment, such deviations are manifest once the probability to measure an event becomes of the order of – or rarer than – one part over one million, hence the crucial importance of a large dataset. The role of finite-Reynolds-number effects and the related fluctuations when pair separations cross the boundary between viscous and inertial range scales are discussed. An asymptotic prediction based on the multifractal theory for inertial range intermittency and valid for large Reynolds numbers is found to agree with the data better than the Richardson theory. The agreement is improved when considering heavy particles, whose inertia filters out viscous scale fluctuations. By using the exit-time statistics we also show that events associated with pairs experiencing unusually slow inertial range separations have a non-self-similar PDF.

Key words: intermittency, multiphase and particle-laden flows, turbulent mixing

1. Introduction

Dispersion of particles in stochastic and turbulent flows is a key fundamental problem (Monin & Yaglom 1975) with applications in a huge number of disciplines ranging from atmospheric and ocean sciences (Bennett 1984; Ollitraut, Gabillet & Colin De Verdiére 2005; Poulain & Zambianchi 2007; Lacorata, Mazzino & Rizza 2008; LaCasce 2010), to environmental sciences (Csanady 1973), chemical

† Email address for correspondence: biferale@roma2.infn.it

engineering and astrophysics (Baldyga & Bourne 1999; Lepreti *et al.* 2012). At high Reynolds numbers, molecular diffusion makes a negligible contribution to spatial transport, and so turbulence dominates not only the transport of momentum, but also that of temperature, humidity, salinity and of any chemical species or concentration field. Mixing can be approached from an Eulerian point of view, studying the spatial and temporal evolution of a concentration field (Dimotakis 2005), and also by using a Lagrangian approach in terms of the relative dispersion of pairs of particles (Falkovich, Gawędzki & Vergassola 2001; Sawford 2001; Salazar & Collins 2009). Notwithstanding the enormous literature on the topic, a stochastic model for particle trajectories in turbulent flows whose basic assumptions are fully justified has yet to arrive (Thomson 1990; Borgas & Sawford 1994; Kurbanmuradov 1997; Borgas & Yeung 2004; Pagnini 2008). The modelling of pair dispersion for tracers was pioneered in Richardson (1926), where a locality assumption was introduced, see also Benzi (2011) for a recent historical review. In a modern language, Richardson's approach is built up in analogy with diffusion, replacing molecular fluctuations with turbulent fluctuations, acting differently at different scales. Hence, in a turbulent flow, diffusivity is enhanced because the instantaneous separation rate depends on the local turbulent conditions encountered by pairs along their path:

$$\frac{\mathrm{d}\langle r^2\rangle}{\mathrm{d}t} = D(r), \quad r_0 \ll r \ll L, \tag{1.1}$$

where $r(t)$ is the amplitude of the separation vector between the two particles, $\boldsymbol{r}(t) = \boldsymbol{X}_1(t) - \boldsymbol{X}_2(t)$, and $D(r)$ is a scalar eddy-diffusivity. For the eddy-diffusivity approach to be valid, separations r have to be chosen larger than the initial ones, r_0, and smaller than the integral scale of the flow, L. Moreover, time lags have to be large enough such that the memory of the initial separation is lost.

In the light of the Kolmogorov 1941 theory, see Frisch (1995), the scalar eddy-diffusivity can be modelled as follows:

$$D(r) \propto \tau(r,t)\langle(\delta_r u)^2\rangle \sim k_0 \epsilon^{1/3} r^{4/3}, \tag{1.2}$$

where $\delta_r u$ is the Eulerian longitudinal velocity difference along the direction of particle separation $\boldsymbol{r}$, $\delta_r u(\boldsymbol{r}(t),t) = \hat{\boldsymbol{r}} \cdot (\boldsymbol{u}(\boldsymbol{X}_1(t),t) - \boldsymbol{u}(\boldsymbol{X}_2(t),t))$, k_0 is a dimensionless constant, and ϵ is the rate of kinetic energy dissipation in the flow. In the above equation, $\tau(r,t)$ is the correlation time of the Lagrangian velocity differences at scale $\boldsymbol{r}$,

$$\tau(r,t) = \frac{2}{\langle[\delta_r u(\boldsymbol{r}(t),t)]^2\rangle} \int_0^t \langle \delta_r \boldsymbol{u}(\boldsymbol{r}(t),t) \cdot \delta_r \boldsymbol{u}(\boldsymbol{r}(s),s)\rangle \mathrm{d}s. \tag{1.3}$$

In the inertial range of scales, by dimensional considerations, we can write $\tau(r) \simeq \epsilon^{-1/3} r^{2/3}$ and $\langle(\delta_r u)^2\rangle \simeq (\epsilon r)^{2/3}$, from which the celebrated Richardson's 4/3 law of (1.2) follows. As a consequence, (1.1) predicts a super-diffusive growth for the particle separation:

$$\langle r^2(t)\rangle \simeq \epsilon t^3, \tag{1.4}$$

and the dependence on the initial conditions is quickly forgotten. In fact, when released into a fluid flow, tracer pairs separate ballistically at short time lags, *à la* Batchelor (Batchelor 1950), keeping memory of their initial longitudinal velocity difference, $\langle r^2(t)\rangle \simeq \langle r_0^2\rangle + C(\epsilon r_0)^{2/3} t^2$, up to time lags of the order of $t_B(r_0) \sim (r_0^2/\epsilon)^{1/3}$. It is only later that Richardson's super-diffusive regime follows.

Richardson's approach is exact if we assume that tracers disperse in a δ-correlated-in-time velocity field. In such a case, the probability density function (PDF) of observing two tracers at separation r at time t, $P(r, t|r_0 t_0)$, satisfies a Fokker–Planck diffusive equation with a space-dependent diffusivity coefficient, $D(r)$ (Kraichnan 1966; Falkovich *et al.* 2001):

$$\frac{\partial P(r,t)}{\partial t} = \frac{1}{r^2}\frac{\partial}{\partial r}\left[r^2 D(r)\frac{\partial P(r,t)}{\partial r}\right], \tag{1.5}$$

where $D(r)$ is a function of the velocity correlation evaluated at the current separation only.

The Richardson equation (1.5) with initial condition $P(r, t_0) \propto \delta(r - r_0)$ can be solved, see e.g. Lundgren (1981) and Bennett (2006), and the solution has an asymptotic, large-time form (independent of the initial condition r_0 and t_0) of the kind:

$$P(r,t) = A\,\frac{r^2}{(k_0\epsilon^{1/3}t)^{9/2}}\,\exp\left[-\frac{9r^{2/3}}{4k_0\epsilon^{1/3}t}\right], \tag{1.6}$$

where A is a normalization constant. The Richardson PDF is perfectly self-similar, so that all positive moments behave according to the dimensional law, $\langle r^p\rangle \propto (\epsilon^{1/3}\,t)^{3p/2}$.

There are many reasons why the Richardson distribution cannot exactly describe the behaviour of tracer pairs in real flows. The most important ones are: (i) the nature of the temporal correlations in the fluid flow (Falkovich *et al.* 2001; Chaves *et al.* 2003); (ii) the non-Gaussian fluctuations of turbulent velocities (Frisch 1995); (iii) the small-scale effects induced by the dissipation sub-range, and (iv) the large-scale effects induced by the flow correlation length. These last two are of course connected to finite-Reynolds-number effects.

It is worth noticing that formally any diffusion coefficient of the form $D(r, t) \sim r^\alpha\, t^\beta$, with $3\alpha + 2\beta = 4$, is compatible with the $\sim t^3$ law; however, different results would then be obtained for the functional form of $P(r, t)$ (Monin & Yaglom 1975).

Since Richardson's seminal work, pair dispersion has been addressed in a large number of experimental and numerical studies, in the 2d inverse energy cascade (Jullien, Paret & Tabeling 1999; Boffetta & Celani 2000; Boffetta & Sokolov 2002*a*) and in the direct enstrophy cascade (see e.g. Jullien 2003), as well as in the 3d direct energy cascade (Ott & Mann 2000; Biferale *et al.* 2005*a*), in convective turbulent flows (Schumacher 2008; Ni & Xia 2013; Mazzitelli *et al.* 2014) and in synthetic flows (Fung & Vassilicos 1998; Malik & Vassilicos 1999; Thomson & Devenish 2005; Nicolleau & Nowakowski 2011). In Sawford, Yeung & Borgas (2005), kinematic and direct numerical simulations (DNS) have also been used to compare forward and backward relative dispersion in three-dimensional turbulent flows. Comprehensive reviews on the topic can be found in Falkovich *et al.* (2001), Sawford (2001) and Salazar & Collins (2009).

Despite the huge amount of theoretical, numerical and experimental works devoted to this issue, it is fair to say that at the moment there is neither a clear consensus in favour of the Richardson's approach, nor a clear disproof. The main practical reason is due to the fact that the predictions – if correct – are applicable to tracer pairs whose evolution has been for all times in the inertial range of scales:

$$\eta \ll r(t') \ll L \quad \forall t' \in [t_0, t], \tag{1.7}$$

where η is the viscous scale of the turbulent flow. In other words, we should record tracer dispersion at space and time scales unaffected by viscous or integral

scale effects. This is of course a strong requirement which is particularly difficult to match in any experimental or numerical test because of the natural limitations in the accessible Reynolds number Re_λ, i.e. in the scale separation range $Re_\lambda \propto (L/\eta)^{2/3}$. Moreover, the viscous scale η itself and the stretching rate at this scale are strongly fluctuating quantities in turbulent flows (Frisch 1995; Schumacher 2007; Yakhot 2006; Biferale 2008), causing further difficulties when pair statistics must be limited to a pure inertial range behaviour. It is worth noticing that a possible way out is to resort to exit-time statistics (Artale *et al.* 1997; Boffetta & Sokolov 2002*a*; Biferale *et al.* 2005*a*), which will be discussed in § 4.

To avoid viscous effects on the pair dispersion statistics, it is also common to study pairs whose initial separation is well inside the inertial range, $r(t_0) \gg \eta$, paying the price of being dominated for long times by the initial condition and therefore mostly accessing the Batchelor regime (Bourgoin *et al.* 2006; Bitane, Homann & Bec 2012*a*). Alternatively, numerical simulations of particles evolving in stochastically generated velocity fields are a useful tool to describe (possibly non-Gaussian and non-self-similar) inertial range pair dispersion (Kurbanmuradov 1997; Boffetta *et al.* 1999; Malik & Vassilicos 1999; Thomson & Devenish 2005). Note, however, that kinematic simulations might lead to a mean-squared separation of the particle pairs with a power law different from the Richardson's law (Thomson & Devenish 2005).

For the reasons (i)–(ii) listed above, it is quite possible that, even in an infinite-Reynolds-number limit, the Richardson's prediction may turn out to be wrong. Effects of time correlations have been discussed by many authors (Klafter, Blumen & Shlesinger 1987; Sokolov 1999; Bitane *et al.* 2012*a*; Scatamacchia, Biferale & Toschi 2012; Eyink 2013), in connection with the problem of the formally admissible infinite propagation speed present in any diffusive approach *à la* Fokker–Planck (Masoliver & Weiss 1996; Kanatani, Ogasawara & Toh 2009; Ilyin, Procaccia & Zagorodny 2013), and also in relation to the possible non-Markovian nature of the Lagrangian position and velocity process (Thalabard, Krstulovic & Bec 2014).

Summarising, it is extremely important to clarify with high accuracy if the deviations from Richardson's theory observed in laboratory experiments and numerical simulations, at finite Reynolds numbers, are due to sub-leading effects associated with the lack of scale-separation or not. In the latter case, it means that they would survive even in the $Re \to \infty$ limit. This is the aim of the research presented in this paper.

We use DNS of isotropic and homogeneous three-dimensional turbulence at $Re_\lambda \sim 300$, seeded with an unprecedented number of particles (emitted from localised sources in different locations inside the flow), in order to increase the total number of pairs starting with an initially small separation and to minimise local anisotropy and non-homogeneity.

We present results for both tracers and point-like heavy particles, without feedback on the flow as in the original problem attacked by Richardson. When particles have inertia, new scenarios arise (Fouxon & Horvai 2008; Bec *et al.* 2010*a*), because of the non-homogeneous spatial distribution (Bec *et al.* 2006*a*) and the very intermittent nature of relative velocity increments characterised by the presence of quasi-singularities (Falkovich, Fouxon & Stepanov 2002; Wilkinson & Mehlig 2005; Bec *et al.* 2010*b*; Pan & Padoan 2010; Bec *et al.* 2011; Salazar & Collins 2012).

Not surprisingly, and in the absence of a theory, empirical observations are in this case even less stringent, also because of the need to specify the initial distributions of both particle positions and velocities. Two types of experiments can be done with inertial particles. The first consists of studying relative dispersion as a function of

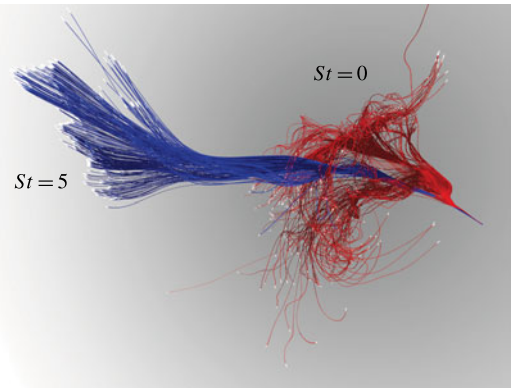

FIGURE 1. (Colour online) An ensemble of tracer particles with $St = 0$ (red) and heavy particles with $St = 5$ (blue), simultaneously emitted from a source of size $\sim \eta$. Trajectories are recorded from the emission time, up to the time $t = 75\tau_\eta$ after the emission.

the distribution of initial separations only. In practice, inertial particles are allowed to reach their stationary spatial and velocity distributions inside a bounded volume (stationary distribution on a fractal dynamical attractor in phase–space), after which their dispersion properties are measured, conditioning on the initial distance (Bec *et al.* 2010*a*). The second consists in directly injecting inertial particles in the flow, with prescribed initial velocity and separation distributions. The first protocol is more relevant to study relative dispersion properties in connection with spatial clustering, particularly effective at small Stokes numbers (e.g. the spatial preferential concentration and trapping in coherent structures in the flow), and in connection with caustics, strongly modifying the relative velocities at large Stokes numbers (Abrahamson 1975; Bec *et al.* 2010*a*,*b*; Pan & Padoan 2010). The second protocol is more relevant in geophysical and industrial applications, where transient behaviours are crucial, as in the case of volcanic eruptions, leakages of contaminants, or pollutant emissions.

In this paper, we are interested in the latter case, for which we designed the simplest procedure of having inertial particles emitted in the same positions and with the same velocities of the tracers (see figure 1). This choice turns out to be optimal to better understand the statistics of tracers also, as it will become clearer in the sequel.

The main results of the paper can be briefly anticipated. First, we quantify the importance of viscous-scale fluctuations for tracer separations, showing that they easily affect the separation evolution for time scales much larger than predicted by the dimensional Batchelor time, $t_B(r_0)$. This effect is so huge that, in current experiments, it ruins any possibility of assessing tracer scaling properties in the expected inertial range of time scales. To overcome this problem, we suggest that heavy pairs can be used as dispersing particles that are able to dynamically filter out viscous-time fluctuations. By measuring pair dispersion of heavy pairs at different degrees of inertia, we are able to observe a much clearer convergence towards an inertial-range regime for the relative separation. We interpret this result as an indication of the existence of infinite-Reynolds-number corrections to the Richardson's prediction, as expected on the basis of a Eulerian–Lagrangian multifractal approach (Borgas 1993; Boffetta *et al.* 1999; Biferale *et al.* 2004), yet never observed in real data. The multifractal (MF) approach is also used to determine a set of specific correlation moments involving powers of the pair separation distance and relative velocity of tracer pairs, which are

expected to be statistically invariant along Lagrangian trajectories in the inertial range (Falkovich *et al.* 2001; Falkovich & Frishman 2013).

The paper is organised as follows. In § 2, we present the details of our numerical study. In § 3, we introduce the relative dispersion statistics for both tracers and heavy particles. In § 3.1, we discuss the effects due to finite Reynolds numbers and those induced by the fluctuations of the viscous scale. In § 3.2, we present the numerical data for the PDFs. In connection with the issue of intermittent corrections, in § 3.3, we briefly review the multifractal prediction for the pair dispersion of tracers developed by Boffetta *et al.* (1999), and we test it against our data. In § 4, we discuss the results concerning the exit-time statistics, probing pairs which separate very slowly.

2. Numerical details

The fluid is described by the Navier–Stokes equations for the velocity field $\boldsymbol{u}(\boldsymbol{x}, t)$

$$\partial_t \boldsymbol{u} + \boldsymbol{u} \cdot \boldsymbol{\nabla} \boldsymbol{u} = -\boldsymbol{\nabla} p + \nu \nabla^2 \boldsymbol{u} + \boldsymbol{f}, \quad \boldsymbol{\nabla} \cdot \boldsymbol{u} = 0. \tag{2.1}$$

The statistically homogeneous and isotropic external forcing $\boldsymbol{f}$ injects energy in the first low-wavenumber shells, by keeping constant in time their spectral content (Chen *et al.* 1993). The kinematic viscosity ν is chosen such that the Kolmogorov length scale is $\eta \simeq \delta x$, where δx is the grid spacing, so that a good resolution of the small-scale velocity dynamics is obtained. The numerical domain is cubic, with periodic boundary conditions in the three space directions; a fully dealiased pseudo-spectral algorithm with second-order Adams–Bashforth time-stepping is used. We performed a series of DNS with a resolution of 1024^3 grid points and a Reynolds number at the Taylor scale $Re_\lambda \simeq 300$. The flow is seeded with bunches of tracers and heavy particles, emitted in different fluid locations to reduce the large-scale correlations and local inhomogeneous/anisotropic effects. Each bunch is emitted within a small region of space, of Kolmogorov-scale size, in puffs of 2×10^3 particles each, for tracers and heavy particles. In a single run there are 256 of such point sources, releasing approximately 80 puffs with a frequency comparable to the inverse of the Kolmogorov time. We collected statistics over 10 different runs. As a result, we follow a total amount of 4×10^{11} pairs.

The heavy particles are assumed to be of size much smaller than the Kolmogorov scale of the flow and with a negligible Reynolds number relative to the particle size. In this limit, their equations of motion take the simple form:

$$\dot{\boldsymbol{X}}(t) = \boldsymbol{V}(t), \quad \dot{\boldsymbol{V}}(t) = -\frac{1}{\tau_s}[\boldsymbol{V}(t) - \boldsymbol{u}(\boldsymbol{X}, t)], \tag{2.2a,b}$$

where the dots denote time derivatives. The particle position and velocity vectors are $\boldsymbol{X}(t)$ and $\boldsymbol{V}(t)$, respectively; $\boldsymbol{u}(\boldsymbol{X}, t)$ is the Eulerian fluid velocity evaluated at the particle position. The particle response time is τ_s. The flow Kolmogorov time scale, appearing in the definition of the Stokes number, $St = \tau_s/\tau_\eta$, is $\tau_\eta = (\nu/\epsilon)^{1/2}$. Particle–particle interactions and the feedback of the particles onto the flow are here neglected. In this work, we show results for the following set of Stokes numbers: $St = 0.0$, 0.6, 1.0 and 5.0. Additional details of the runs can be found in table 1.

3. Relative separation statistics

In figure 1, we compare the time evolution up to a time of the order of the large-scale eddy turnover time, T_E, of a bunch of tracers and a bunch of heavy particles with $St = 5$, both emitted in a region of strong shear.

Re_λ	N^3	η	Δx	ϵ	ν	τ_η	T_E	u_{rms}	N_p	N_{sou}	N_{tot}	T_{traj}
280	1024^3	0.005	0.006	0.81	0.00088	0.033	67	1.7	2×10^3	256	4×10^{11}	160

TABLE 1. Parameters of the numerical simulations: Taylor-scale-based Reynolds number Re_λ, grid resolution N^3, Kolmogorov length scale η in simulation units (SU), grid spacing Δx (SU), mean energy dissipation ϵ (SU), kinematic viscosity ν (SU), Kolmogorov time scale τ_η (SU), large-scale eddy turnover time T_E (in units of τ_η), root-mean-square velocity u_{rms} (SU), N_p number of trajectories of inertial particles emitted for each Stokes number St from each local source and for each puff, N_{sou} number of sources in the flow, N_{tot} total number of particle pairs emitted in all simulations per Stokes number (10 runs with 256 local sources, each emitting 80 puffs), T_{traj} maximal temporal length of particle trajectories (in units of τ_η).

At a time lag roughly equal to $t = 10\tau_\eta$ after the emission, an abrupt transition in the particle dispersion of tracers (red in the online version) can be observed, occurring when most of the pairs reach a relative distance of the order of 10η. Later, we again notice the presence of many pairs with mutual separations much larger than the mean value. The trajectories of the heavy particles (blue in the online version) show a different evolution. After the emission, they tend to remain at a mutual distance of the order of η for a very long time, thus dispersing much less. Because they respond to fluid fluctuations with a time lag of the order of their Stokes time, they tend to keep their initial velocity unchanged before relaxing to the underlying fluid velocities. As a result, inertial particles behave as if their Batchelor time was much longer than that of tracers (in our DNS the latter is small, $t_B(r_0, St = 0) \sim \tau_\eta$, because the source is strongly localised). Our main observation here is that the larger the Stokes number, the longer is the filtering time that heavy particles apply to the local stretching properties of the carrying fluid: since inertia is moderate in the present experiment, this fact will allow us to have a very effective method to reduce effects from viscous-scale fluctuations in the particle statistics and to better disentangle inertial range properties in the pair dispersion evolution.

This is more quantitatively understood in figure 2, where the second-order moments of the relative separation for tracers, $St = 0$, and heavy particles, $St = 5$, are plotted. Heavy particles tend to separate less since they are unaffected by turbulent fluctuations up to time and spatial scales large enough for their inertia to become sub-dominant with respect to the underlying turbulent fluctuations. On dimensional grounds, such a scale can be easily estimated to be of the order of $r^*(St) \sim \eta St^{3/2}$ when $St > 1$ (Bec *et al.* 2010*a*). Let us notice that in this respect the choice of the initially prescribed velocity distribution plays a key role, since inertial particles are emitted with a velocity equal to that of the underlying fluid. The quantity which is better suited to quantify this observation is the ratio between relative separations:

$$Q(t) = \frac{\langle r^2(t) \rangle_{St}}{\langle r^2(t) \rangle_0}. \tag{3.1}$$

In the present experiment we observe $Q(t) < 1$ at any scale and time, as shown in the lower inset of figure 2. By prescribing an initial distribution equal to the stationary PDF of heavy particle velocity increments, the trend would have been the opposite, with inertial particles at short times separating much faster than tracers, i.e. $Q(t) > 1$ up to a separation $r \simeq r^*(St)$ (Bec *et al.* 2010*b*). In the main body of figure 2, we

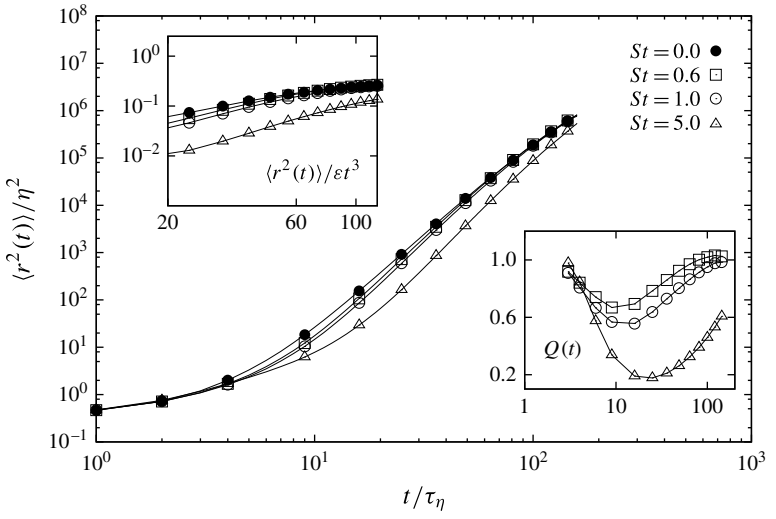

FIGURE 2. (Main body) Log–log plot of the mean-squared separation versus time for particle pairs at changing inertia. (Upper inset) Log–log plot of the same curves, compensated with the Richardson's inertial range behaviour. (Lower inset) The ratio $Q(t)$, on a log–lin scale, of the mean-squared separation of heavy particle pairs, normalised with the curve for tracer pairs.

notice that for both tracers and heavy particles, and for time lags large enough, the separation curves tend toward a t^3 Richardson-like behaviour, but without showing any clear scaling, as also measured by the compensated plot in the upper inset of figure 2.

3.1. *Viscous effects*

To better appreciate the importance of viscous effects on pair dispersion, in figure 3 we show the time evolution of two different bunches of tracers emitted in different positions in the flow. The initial size of the puffs is of the order of the viscous scale. The bunch on the left is emitted in a region where the stretching rate has a typical value of the order of its root mean square, $\sim(\epsilon/\nu)^{-1/2}$, while the bunch on the right is emitted in a region where the local stretching rate is unusually small. As a result, this second bunch separates with a much longer delay with respect to the average behaviour.

In figure 4, the mean-squared separations measured for pairs belonging to each of these two bunches are compared with the pair separation averaged over the full statistics. The bunch emitted in a region where the stretching rate assumes the typical value exits the viscous region in a time lag of the order of τ_η, and soon approaches the inertial range behaviour compatible with $\sim t^3$. Pairs belonging to the other bunch keep a small separation $\langle r^2\rangle^{1/2} \simeq \eta$ for a time lag up to $\sim 50\tau_\eta$, a time comparable to the integral time scale T_E, and never recover the t^3 scaling behaviour along the whole duration of our simulation. The examples shown in figure 4 are meant to represent the huge variations that affect pair separation statistics for time lags of the order of τ_η. These variations are the most difficult obstacle in assessing pure inertial range properties in any experimental or numerical set-up, in addition to the challenge of following particle trajectories for a sufficiently long time lag – in a sufficiently large volume.

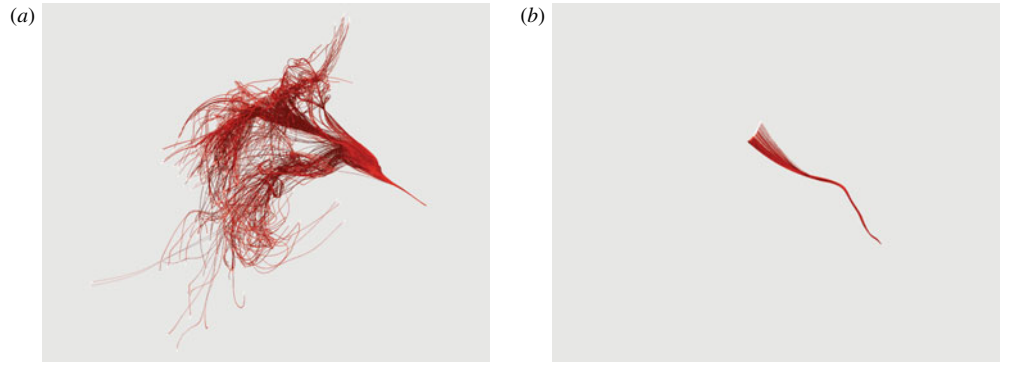

FIGURE 3. (Colour online) (*a*): the same ensemble of tracers reported in figure 1. (*b*): simultaneous realisation of a tracer bunch, emitted from a different source, showing a much smaller dispersion. Both emissions are recorded up to the time $t = 75\tau_\eta$.

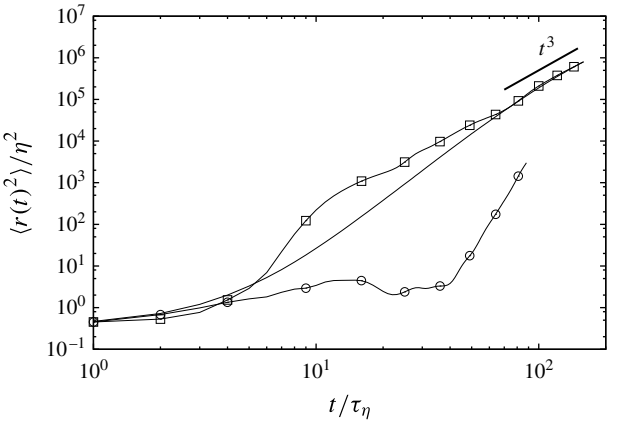

FIGURE 4. The mean-squared separation behaviour for the two tracer emissions reported in figure 3. Data from the left panel are represented by (□); while data from the right panel are represented by (○). The continuous curve is the mean-squared separation averaged over the whole statistical database.

Our idea here is to use heavy particles as smart passive, but dynamical, objects to filter out such huge viscous effects, without affecting the long-time and large-scale physics. Indeed, heavy particles are less affected by fluctuations of the local viscous scale, since they respond to the fluid with their Stokes time (see figure 1). Moreover, heavy pairs experience a less fluctuating local stretching rate, as also measured by the distribution of the finite-time Lyapunov exponents as a function of the Stokes number (Bec *et al.* 2006*b*). Finally, we recall that, because of the injection choice here adopted, caustics in the heavy particles velocity distribution manifest themselves only at a later stage. As for the heavy pairs dispersion, the different degrees of fluctuations are better quantified in figure 5, where we show the ratio of the third- and fourth-order moments of the separation distribution along the particle trajectories, normalised by the second-order moment

$$F_3(t) = \frac{\langle r^3(t) \rangle}{\langle r^2(t) \rangle^{3/2}}; \quad F_4(t) = \frac{\langle r^4(t) \rangle}{\langle r^2(t) \rangle^2}. \tag{3.2a,b}$$

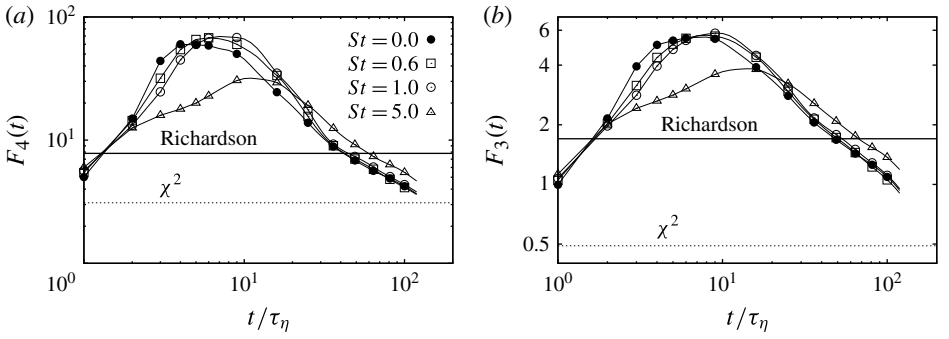

FIGURE 5. Generalised flatness (*a*) and skewness (*b*) of the relative dispersion PDF, for pairs of different inertia. Horizontal lines refer to the Richardson expectations for these observable, which are 7.81 and 1.7, respectively; also plotted are the expected values for a χ-squared distribution with three degrees of freedom, which are 3.1 for the flatness and 0.49 for the skewness.

For convenience, we refer to $F_3(t)$ and $F_4(t)$ as generalised skewness and flatness, respectively. At the transition between the viscous and the inertial range of scales, i.e. for $t \simeq 10\tau_\eta$, tracers and small Stokes particles possess a generalised flatness $F_4(t) \sim 100$. This is the signature of an extremely intermittent distribution (for a χ-squared distribution with three degrees of freedom, we would have $F_4 = 3.1$, while for the Richardson distribution $F_4 = 7.81$). Moreover, it is evident that the bump displayed by the generalised flatness around $10\tau_\eta$ is influenced by the behaviour at shorter times and influences the behaviour at much larger times. In other words, it is the quantitative counterpart of the large variations shown in the two examples in figure 4.

The filtering effect of the particle Stokes time is the reason for which heavy pairs initially possess a smaller flatness. This is particularly evident for the $St = 5$ case, which exhibits a smoother transition towards a scaling behaviour for $t > 10 - 20\tau_\eta$, supporting the idea the inertia helps to remove viscous fluctuations from the physics of the inertial range. At time lags $20\tau_\eta$, the generalised coefficients $F_3(t)$ and $F_4(t)$ for heavy particles with $St = 5$ are larger than those of the tracer pairs. This is probably the result of the relaxation onto the tracer power-law behaviour, which happens only at a later stage. Finally, it is clear from figure 5 that the data set at the moderate inertia of $St = 5$ is less affected by the strong viscous bump at $t \sim 10\tau_\eta$ and that, therefore, promises to be the best candidate to test inertial range statistical properties.

3.2. *Probability density functions*

The PDFs $P(r, t)$ are plotted in figure 6, for different values of inertia $St = 0$, 0.6, 1 and 5, and at different time lags after the emission from the source. In order to highlight the dynamics of those particles filling the left tail (i.e. separating less than the average), for figure 6 we have selected pairs with initial separation $r(t_0) \in [0.2 : 2]\eta$ (Bitane, Homann & Bec 2012*b*). Consider first the behaviour at large separations. One clearly sees the effect anticipated earlier. Heavy particles tend to separate less. The effect becomes less and less visible with time, because inertia is forgotten on a time scale roughly proportional to the Stokes time. Pairs with $St = 5$, however, accumulate a delay in separation that is never recovered, even at large times $t \sim 50\tau_\eta$.

For the left tails, associated with pairs that do not separate, the trend as a function of Stokes is the opposite. We recall from classical arguments (Falkovich *et al.* 2001)

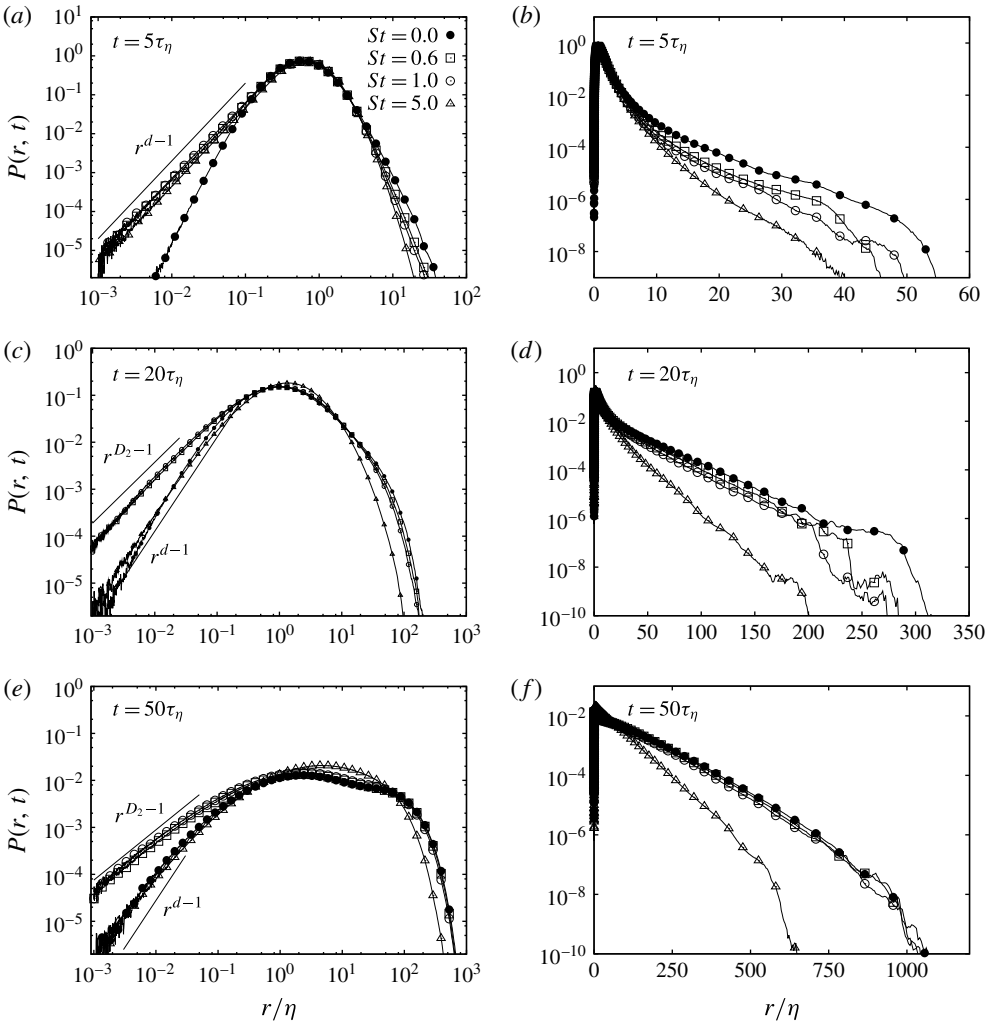

FIGURE 6. (*a*,*c*,*e*) Log–log plot of separation PDFs $P(r, t)$ for pairs with different inertia $St = 0.0, 0.6, 1.0, 5.0$ highlighting the left-tails behaviour. Plots refer to times $5\tau_\eta$, $20\tau_\eta$ and $50\tau_\eta$ after the emission. The power-law scaling r^{d-1}, with $d = 3$, is plotted. The power-law scaling r^{D_2-1} is also reported: note that for $St = 0.6$ the correlation dimension $D_2(St)$ is 2.27 ± 0.03, while for $St = 1.0$ it is $D_2(St) = 2.31 \pm 0.03$ (Bec *et al.* 2011). The two power laws r^{D_2-1} for $St = 0.6$ and $St = 1.0$ are indistinguishable in the scale of the plot, hence we reported the slope for $St = 1.0$ only. (*b*,*d*,*f*): lin–log plot of the same separation PDFs, at the same time lags. For these PDFs pairs are selected with initial separation $r_0 \in [0.2 : 2]\eta$.

that we expect the fraction of tracer pairs at a distance r to behave as a power law r^{d-1}, where $d = 3$ is the space dimension, see (1.6). Similarly, for heavy pairs, we expect to observe the scaling $P(r) \propto r^{D_2-1}$, where $D_2(St) \neq d$ measures the spatial correlation dimension. At short time lags, $t \simeq 5\tau_\eta$, the effect of inertia quickly appears and we measure a higher probability to observe pairs at very small separations: this happens because heavy pairs are less affected than tracers by intermittent events of anomalously slow separations, and hence rapidly populate the left tail of the distribution. As time goes on, $t \simeq 20\tau_\eta$, we observe that pairs with moderate inertia,

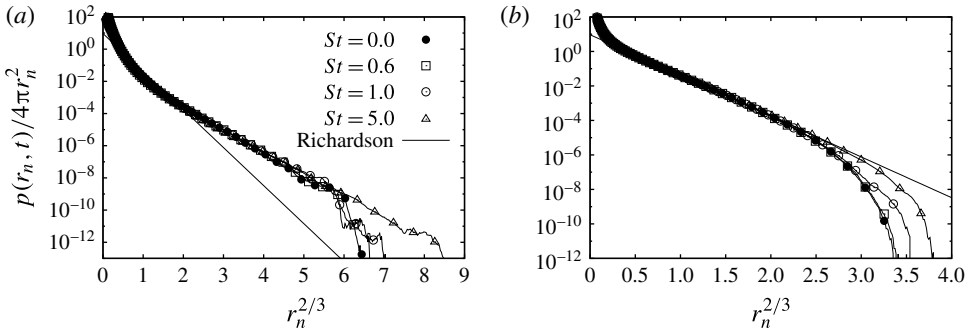

FIGURE 7. Lin–log plot of the pair separation PDFs in rescaled units, $r_n = r/\langle r^2(t)\rangle^{1/2}$, at time lags $20\tau_\eta$ (*a*) and $80\tau_\eta$ (*b*), for different Stokes numbers.

namely $St = 0.6$ and $St = 1$, clearly show the tendency to cluster on a fractal set (Balkovsky, Falkovich & Fouxon 2001; Boffetta, De Lillo & Gamba 2004; Bec 2005; Chun *et al.* 2005; Bec *et al.* 2006*a*) characterised by the spatial correlation dimension $D_2(St) < d$ (Bec *et al.* 2006*a*, 2007), where d is the spatial dimension of the flow. Differently, we clearly observe that the left tail of the tracer PDF superposes well with that of the largest Stokes, $St = 5$: this is because the correlation dimension for this high Stokes number is $D_2(St = 5) \simeq d$. At a later time lag, $t \simeq 50\tau_\eta$, it is very hard to detect a power-law scaling in the left tail, even with the large database of the present experiment: by this time lag, most of the pairs have reached larger separations. Since pair dispersion takes place at finite Reynolds numbers, it is clear that asymptotic power-law behaviours, see (1.6), can be observed in a limited range of space and time scales only. To summarise, the observed power-law scalings at small separations reproduce the classical expectations for tracers and heavy pairs reported in Falkovich *et al.* (2001), and based on the Richardson's model. To detect intermittency effects, which we expect to be present due to tracer pairs that separate much less than the average, different observables are needed. This will be the object of the exit-time analysis in the final section.

Things become more interesting when the pair separation distributions are plotted in dimensionless units. In figure 7, we show the PDFs measured over the whole statistical database, as a function of the pair distance and also in terms of the normalised relative separation,

$$r_n = \frac{r}{\langle r^2(t)\rangle_{St}^{1/2}}. \tag{3.3}$$

It is important to notice that the differences as a function of the Stokes number previously observed are fully reabsorbed once dimensionless quantities are used. This supports a strong universality for large separations as a function of St, at least up to the values here studied. Should the PDF data follow the Richardson's prediction, we would see a perfect rescaling on a stretched exponential curve, for all times and all separations. It is evident that this is not the case. Moreover, we stress that the most important departures from the Richardson's prediction develop on the far right tails, i.e. for intense fluctuations due to pairs that separate much more than the average. This fact has already been observed by Scatamacchia *et al.* (2012) using the same dataset. Previous numerical and experimental studies were limited to events with a probability greater than 10^{-6} (see e.g. Ott & Mann 2000 and Biferale *et al.* 2005*a*), where departures from the Richardson's prediction could not be unambiguously detected.

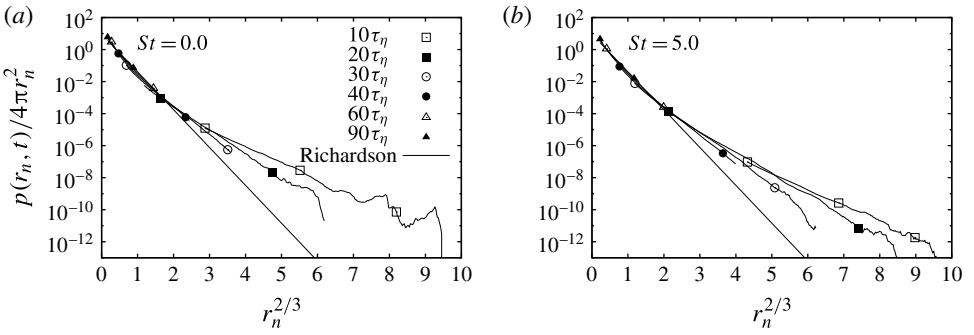

FIGURE 8. Lin–log plot of the rescaled pair separation PDFs at times lags $t = (10, 20, 30, 40, 60, 90)\tau_\eta$, selecting the pair distances to be in the range $r \in [25, 300]\eta$. (*a*) is for tracers, while (*b*) is for heavy pairs with $St = 5$. Symbols are drawn for a subset of points only for clarity.

It must be noticed that the renormalisation in terms of the separation r_n brings some extra difficulties in the interpretation of data. Indeed, since the mean-squared separation, $\langle r^2(t)\rangle_{St}^{1/2}$, is increasing with time, at large times it might well happen that the far right tails of the PDFs are completely dominated by large-scale effects, $r \sim L$. The opposite happens for the events close to the peak, which can be affected by viscous contributions, $r \sim \eta$, for small times. In both cases, finite-Reynolds-number effects come into play. As a result, these rescalings do not allow straightforward conclusions, either to confirm or exclude the alleged departures from the distribution predicted by Richardson in the infinite-Reynolds-number limit.

In figure 8 we show the same data as figure 7, but conditioning the relative separation to belong to the inertial range of scales, $25\eta < r < 300\eta$. A more coherent picture now emerges, since we note that (i) curves belonging to different time lags develop clearly non-overlapping tails; (ii) for times large enough, a universal, Stokes-independent regime seems to develop; (iii) the rapid fall-off of the left tails of the PDFs for extreme separations disappears. These observations suggest the possibility of identifying inertial range statistical properties that show a Reynolds-independent departure from the Richardson's prediction and that cannot be attributed to viscous or large-scale effects.

3.3. *The multifractal prediction for pair dispersion*

The presence of inertial-range deviations from the pure self-similar behaviour of pair separation statistics predicted by the Richardson's approach should not be surprising, although never observed. In the 3d direct energy cascade regime, anomalous scaling is measured both in the statistics of Eulerian longitudinal and transverse velocity increments (Frisch 1995; Sreenivasan & Antonia 1997; Biferale, Lanotte & Toschi 2008), and in the statistics of Lagrangian velocity increments along single particle trajectories (Mordant *et al.* 2001; Biferale *et al.* 2004; Xu *et al.* 2006; Arneodo *et al.* 2008; Biferale, Calzavarini & Toschi 2011). A simple argument predicts the presence of intermittent corrections in the high-order moments of the relative particle separation, $\langle r^p\rangle$ (Novikov 1989; Boffetta *et al.* 1999). The starting point is the exact relation for the moment of order p of the pair separation,

$$\frac{\mathrm{d}}{\mathrm{d}t}\langle r^p\rangle = p\langle r^{p-1}(\delta_r u)\rangle, \tag{3.4}$$

where $\delta_r u$ is the velocity increment measured along the tracer pair trajectories, separated by a distance r. Here, for simplicity, we have neglected the tensorial structure and the time dependency of r and $\delta_r u$ is understood. Let us suppose that the above correlation can be estimated with fully Eulerian quantities, then the MF approach (Frisch 1995) could be employed to obtain:

$$\langle r^{p-1}(\delta_r u)\rangle \propto \int \mathrm{d}h\, r^{3-D(h)} r^{p-1} r^h, \tag{3.5}$$

where $P(h) \propto r^{3-D(h)}$ is the probability of observing an Eulerian velocity fluctuation at the scale r with a local scaling exponent h, $\delta_r u \sim r^h$, as a function of the spectrum of fractal dimension, $D(h)$. In order to relate the above Eulerian estimate with the Lagrangian estimate in (3.4), one can adopt the dimensional bridge relation supposing that Lagrangian velocity fluctuations at separation $r(t)$ are connected to Eulerian spatial fluctuations at scale r with $t \sim r/\delta_r u \sim r^{1-h}$. This amounts to saying that one can use the same fractal dimensions $D(h)$ for the Lagrangian and Eulerian velocity statistics. A quantitative support for this hypothesis has been made by a validation for one-particle quantities against numerical and experimental results in Arneodo *et al.* (2008). The same argument applied to two-particle quantities allows one to rewrite (3.5) as a function of the time lag, t, along the particle separations,

$$\langle r^{p-1}(\delta_r u)\rangle \propto \int \mathrm{d}h\, t^{((2-D(h)+p+h)/(1-h))}. \tag{3.6}$$

After time integration, a saddle-point approximation can be used in the limit $t \to 0$, when the smallest exponent dominates the integral (Boffetta *et al.* 1999):

$$\langle r^p(t)\rangle \propto t^{\alpha(p)}, \quad \alpha(p) = \min_h \frac{(3 - D(h) + p)}{(1-h)}. \tag{3.7}$$

This is the multifractal theory for tracer pair separation statistics in the presence of an Eulerian velocity field (Boffetta *et al.* 1999), whose multiscale statistics is described by the set of fractal dimension $D(h)$. To our knowledge, such a prediction has never been tested, either on experimental or on numerical data, except for the validation against stochastic velocity fields reported in Boffetta *et al.* (1999). Note that the multifractal spectrum is in general nonlinear in the order p; since by the 4/5-law, the exponent of the third-order longitudinal Eulerian structure function must be unity, we must also have that $\alpha(2) \equiv 3$ (Novikov 1989; Boffetta *et al.* 1999). In figure 9, we compare the multifractal spectrum, $\alpha(p)$, obtained by using two possible forms for $D(h)$ (extracted from the longitudinal and transverse Eulerian structure functions, $D_L(h)$ and $D_T(h)$, respectively) in statistically homogeneous and isotropic 3d turbulence. Such a small uncertainty is to be considered as our prediction error on the shape of the function $D(h)$, which cannot be deduced by first principles. A more detailed discussion about this point can be found in Benzi *et al.* (2010).

To measure the scaling behaviours, we use the procedure known as extended self-similarity (ESS) (Benzi *et al.* 1993), which amounts to studying the relative scaling of moments with respect to a reference moment, whose exponent is constrained by an exact relation. In figure 10, the pth-order moment of particle separation is compensated with the second-order moment:

$$F_p(t) = \frac{\langle r^p(t)\rangle}{\langle r^2(t)\rangle^{(\alpha(p)/3)}}, \tag{3.8}$$

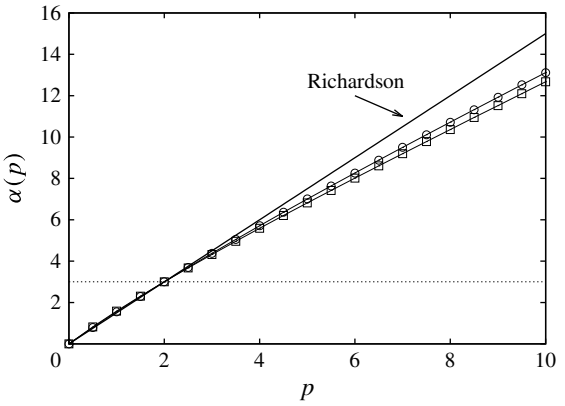

FIGURE 9. Multifractal exponents for pair separation statistics, derived from the scaling exponents of the Eulerian longitudinal structure functions, $D_L(h)$ (○), and from the scaling exponents of Eulerian transversal structure functions, $D_T(h)$ (□). The continuous line is the dimensional Richardson scaling, $\alpha(p) = 3p/2$.

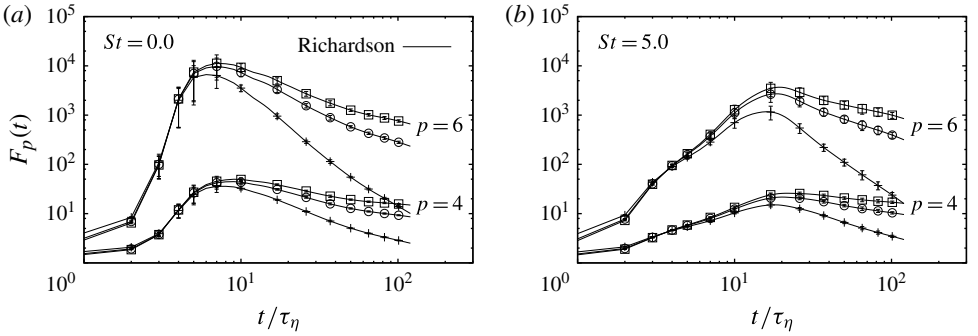

FIGURE 10. The ratio of pair separation moments of order $p = 4$ and $p = 6$ to the second-order moment, as a function of time. For each moment, the upper curve is obtained by compensating with the multifractal exponent, $\alpha(p)$, obtained from the Eulerian transverse structure functions, while the middle curve is obtained by compensating with the multifractal exponent from the Eulerian longitudinal structure functions (see previous figure and discussion in the text). The lower curve is obtained by compensating with the Richardson's dimensional scaling $\alpha(p) = 3p/2$. (*a*) Moments of tracer separation; (*b*) moments of separation of heavy pairs with $St = 5$. The error bars are given by the root mean square of (3.8) computed on two equal subensembles of the whole statistics.

both for tracer pairs and for heavy pairs at $St = 5$. In the inertial range, where the prediction of (3.7) is expected to be valid, we should observe a plateau. It is evident that the multifractal prediction works better than the dimensional one, suggesting that the approach goes in the right direction. However, because the plateau is very narrow it is necessary to wait for data at higher Reynolds numbers before making any firm conclusion. The claim is that the observed departure from the multifractal prediction in the tracer statistics is due to contamination induced by viscous effects, which we have seen to be very strong for the $St = 0$ case. The situation becomes more interesting for heavy particles at $St = 5$, for which viscous effects have a smaller impact. Here the multifractal scaling gives a larger plateau for the $p = 4$ moment, and shows the

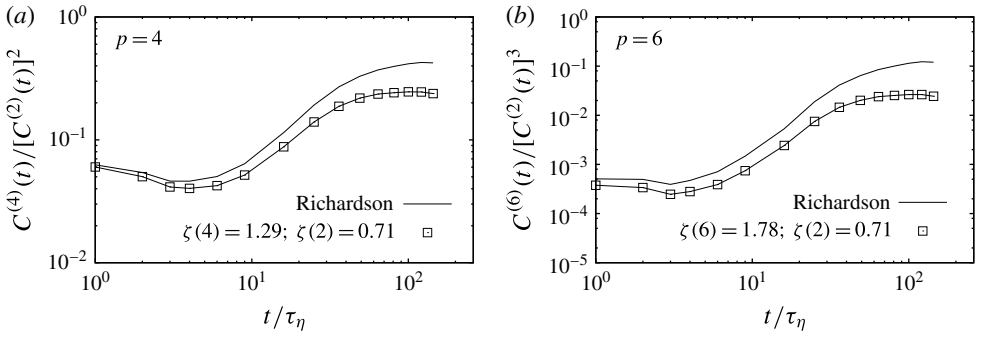

FIGURE 11. The ratio of mixed separation-velocity correlations $C^{(p)}(t)$ of order $p = 6$ and $p = 4$, with respect to a reference order, $C^{(2)}(t)$, versus time. The moments are compensated with the dimensional prediction of the theory of Richardson, and with the longitudinal intermittent scaling exponents.

beginning of a plateau for the $p = 6$ moment. We thus have an indication of an inertial-range intermittent effect for particle pair separation statistics in homogeneous and isotropic 3d turbulence.

This is the main result of this paper.

On the basis of the multifractal formalism, it is straightforward to conclude that there exist correlation functions that should be statistically preserved along pair trajectories for scales well within the inertial range (Falkovich *et al.* 2001; Falkovich & Frishman 2013). Indeed, by again applying the saddle-point estimate to the inertial range scaling of the mixed separation-velocity moments, according to multifractal model we get that

$$C^{(p)}(t) = \langle r(t)^{-\zeta(p)} (\delta_{r(t)} u)^p \rangle \sim \text{const.} \tag{3.9}$$

if the scaling exponents of the particle separation compensate that of the Eulerian velocity moment: $\zeta(p) \equiv \min_h(ph + 3 - D(h))$. In figure 11, we measure the mixed separation-velocity correlations of order $p = 4$ and $p = 6$ in ESS – that is, with reference to the moment of order two. The scaling obtained by using the $\zeta(p)$ exponents is the one that works better for inertial range time lags, i.e. $t > 20\tau_\eta$.

4. Exit-time statistics for tracers

Another interesting question concerns the statistical properties of weak separation events, i.e. the left tail of the PDF. In order to assess the importance of these events, one cannot resort to negative moments of the separation statistics, because these are ill defined. An alternative approach which overcomes this difficulty is to use inverse statistics, see Jensen (1999), i.e. exit times. Exit times also allow for a clearer separation of scales, as stressed by Boffetta & Sokolov (2002*b*). The idea consists in fixing a set of thresholds, $r_n = \rho^n r_0$ with $n = 1, 2, 3, \ldots$ and $\rho > 1$, and calculating the PDF of the time $T(r_n)$ needed for the pair separation to change from r_n to r_{n+1}. Formally this corresponds to calculating the first-passage time. The advantage of this approach is that all pairs are sampled when they belong to eddies of similar size, between r_n and r_{n+1}. This limits the effect of pairs that at a given time lag – since they have separated very fast or very slow – might be at very different separation scales. In other words, in the exit-time statistics the contamination from viscous and large-scale cut-offs should be less important.

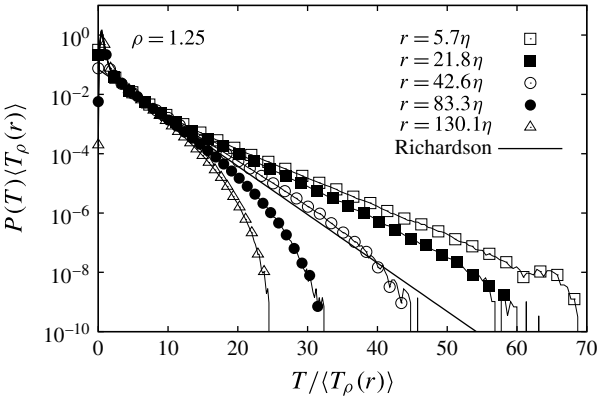

FIGURE 12. The exit-time PDFs for tracer pairs are shown, together with the Richardson's asymptotic form of the exit-time distribution. The growth factors for spatial thresholds is $\rho = 1.25$. The continuous straight line is the Richardson's prediction.

For particle pairs with initial condition $P(r, t=0) = \rho^2 \delta(r - r_n/\rho)/4\pi r_n^2$, a perfectly reflecting boundary condition at $r = 0$ and an absorbing boundary condition at $r = r_n$, the PDF of exit time, $P(T)$, is given by:

$$\mathscr{P}_{\rho,r_n}(T) = -\frac{\mathrm{d}}{\mathrm{d}t} \int_{|\boldsymbol{r}|<r_n} P(\boldsymbol{r}, t)\mathrm{d}\boldsymbol{r}. \tag{4.1}$$

Using the Richardson's distribution of (1.6) for $P(\boldsymbol{r}, t)$, we get

$$\mathscr{P}_{\rho,r_n}(T) = -4\pi k_0 \epsilon^{1/3} r_n^{10/3} \partial_r P|_{r=r_n}. \tag{4.2}$$

An asymptotic form of exit-time PDF behaves according to the following expression,

$$\mathscr{P}_{\rho,r_n}(T) \simeq \exp\left[-\kappa \, \frac{\rho^{2/3} - 1}{\rho^{2/3}} \, \frac{T}{\langle T_\rho(r_n)\rangle}\right], \tag{4.3}$$

where $\kappa \simeq 2.72$ is a dimensionless constant, for details see Biferale *et al.* (2005*a*), and $\langle T_\rho(r_n)\rangle$ is the mean exit time. Note that (4.3) contains only dimensionless parameters and is thus a universal result. We note that while positive moments $\langle T_\rho^p(r_n)\rangle$ preferably sample pairs that separate slowly, negative moments, $\langle [1/T_\rho(r_n)]^p\rangle$, are dominated by pairs that separate fast, Boffetta & Sokolov (2002*b*). From (4.3), a prediction can be obtained for the mean exit time (Boffetta & Sokolov 2002*b*),

$$\langle T_\rho(r)\rangle = \frac{1}{2\,k_0\,\epsilon^{1/3}} \frac{(\rho^{2/3} - 1)}{\rho^{2/3}} \, r^{2/3}, \tag{4.4}$$

from which it follows that, according to the Richardson self-similar behaviour, we expect

$$\langle T_\rho^p(r)\rangle \propto r^{2p/3}. \tag{4.5}$$

In figure 12, we plot the exit-time PDFs for the tracer pairs, calculated for $\rho = 1.25$. First, let us notice that the super-exponential decay observed for the large-distance case is probably due to a systematic bias induced by the fact that we have a finite length in the trajectories and therefore very long exit times cannot be measured. Second, we observe that the curves do not overlap, meaning that the PDFs are not self-similar. Concerning the statistical accuracy, this result is a clear improvement

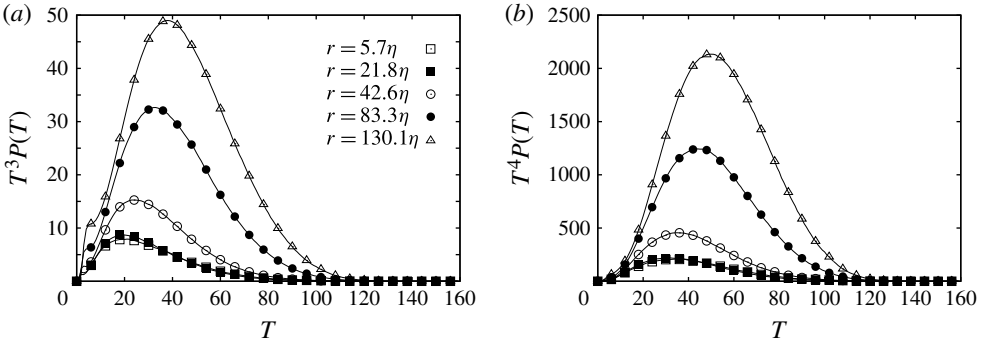

FIGURE 13. Products $T_\rho^p P(T_\rho)$ with $p = 3$ (*a*) and $p = 4$ (*b*) for $\rho = 1.25$, testing the statistical convergence.

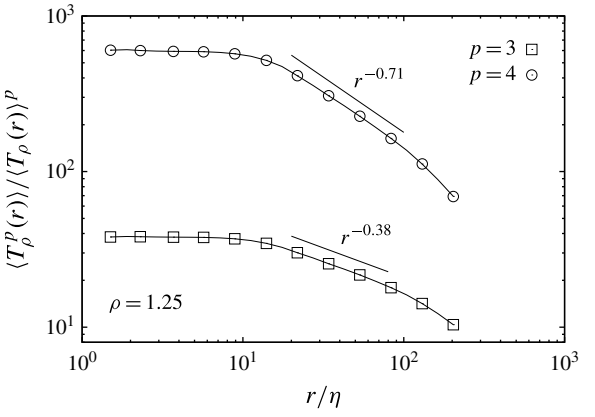

FIGURE 14. The ratio of positive exit-time moments of order $p = 3$ and $p = 4$ to $\langle T_\rho(r)\rangle^p$, as a function of thresholds for $\rho = 1.25$. For different values of ρ we observe the same behaviours.

on that reported in Biferale *et al.* (2005*a*): now deviations from the Richardson's prediction are evident because of the huge statistics achieved in the present numerical experiment. Even though the asymptotic distribution is still given by an exponential decay, as should be expected from rare events following a Poissonian process, the whole PDF shape cannot be superposed using only the mean exit time as a normalising factor.

Concerning the positive moments of the exit times, we use relative scaling properties to test a breaking of the self-similar properties. In figure 13, we verify that we have the statistical convergence needed to measure moments of order $\langle T_\rho^3(r)\rangle$ and $\langle T_\rho^4(r)\rangle$. In figure 14, we show the ratio of $T_\rho(r)$ moments of order $p = 3, 4$ with respect to $\langle T_\rho(r)\rangle^p$, for $\rho = 1.25$. For separations within the inertial range $r/\eta > O(10)$ the breaking of self-similarity is evident. It is difficult to conclude if these are true Reynolds-independent corrections, and if they are affected by the finite length of the particle trajectories. More data will be needed to get a more quantitative understanding of this effect. Furthermore, we recall that there is no multifractal prediction for the behaviour of the positive exit-time moments of relative dispersion, since these would be associated with the negative moments of the Eulerian velocity increments (Jensen 1999).

5. Conclusions

In this work we have numerically studied the relative dispersion statistics of tracer and heavy particles emitted from point-like sources in a homogeneous and isotropic turbulent flow, at resolution 1024^3. When particles are injected at separations of the order of the viscous scale, the fluctuations of the local stretching rate have a huge impact, influencing the mean-squared separation, up to time lags of the order of the integral time scale. Such a dramatic effect has hindered the possibility of studying inertial range quantities in Lagrangian experiments or numerical simulations up to now. In this study, the large statistical database, the use of conditional statistics and the information obtained by comparing tracers and inertial particle evolution enabled us to highlight with a great precision, and for the first time, deviations in the pair separation distribution from the self-similar behaviour predicted by Richardson. Such deviations are manifest in the statistical behaviour of the right tail of the separation PDF, and are due to tracer pairs that separate much faster than the average. We use similar measurements for heavy particles at moderate inertia, which filter out fluctuations of the viscous scales, to give a higher confidence that the corrections observed for tracers are pure inertial range effects. Moreover, by conditioning the relative separation to belong to the inertial range of scales, a universal behaviour develops, which is Stokes independent and is clearly different from the Richardson's prediction. The behaviour of the conditioned PDFs supports the idea that finite-Reynolds-number effects, even if present, are sub-dominant. Furthermore, the numerical results indicate that tracer dispersion is intermittent, with deviations from a self-similar scaling visible already in the low-order moments behaviour. The observed intermittent corrections to the Richardson's prediction are qualitatively consistent with a multifractal prediction for the scaling behaviour of relative separation moments of tracer pairs, although in a narrow scaling region. Numerical and experimental results at higher Reynolds number are required to further support these findings. By measuring the exit-time statistics, we also provide evidence of the non-self-similar character of slow pair dispersion events. The statistics of the shapes of the puffs along the temporal evolution is also a crucial point that is worth studying, involving more information about the multi-particle separation connected to geometry and shapes (Chertkov, Pumir & Shraiman 1999; Biferale *et al.* 2005*b*; Xu, Pumir & Bodenschatz 2011).

Acknowledgements

We thank J. Bec and G. Eyink for useful discussions. We acknowledge financial support from EU-COST Action MP0806 'Particles in Turbulence'. This work is part of the research program of the Foundation for Fundamental Research on Matter (FOM), which is part of the Netherlands Organisation for Scientific Research (NWO). Numerical simulations were performed within the HPC Iscra Class A projects 'Point' and 'Flag' at CINECA (Italy). L.B. acknowledges partial funding from the European Research Council under the European Community's Seventh Framework Programme, ERC Grant Agreement N. 339032.

REFERENCES

ABRAHAMSON, J. 1975 Collision rates of small particles in a vigorously turbulent fluid. *Chem. Engng Sci.* **30**, 1371–1379.

ARNEODO, A., CASTAING, B., CENCINI, M., CHEVILLARD, L., FISHER, R. T., GRAUER, R., HOMANN, H., LAMB, D., LANOTTE, A. S., LÉVÈQUE, E., LÜTHI, B., MANN, J., MORDANT, N., MÜLLER, W.-C., OTT, S., OUELLETTE, N. T., PINTON, J.-F., POPE, S. B., ROUX, S. G., TOSCHI, F., XU, H. & YEUNG, P. K. 2008 Universal intermittent properties of particle trajectories in highly turbulent flows. *Phys. Rev. Lett.* **100**, 254504.

ARTALE, V., BOFFETTA, G., CELANI, A., CENCINI, M. & VULPIANI, A. 1997 Dispersion of passive tracers in closed basins: beyond the diffusion coefficient. *Phys. Fluids* **9**, 3162–3171.

BALDYGA, J. & BOURNE, J. R. 1999 *Turbulent Mixing and Chemical Reactions*. Wiley.

BALKOVSKY, E., FALKOVICH, G. & FOUXON, A. 2001 Intermittent distribution of inertial particles in turbulent flows. *Phys. Rev. Lett.* **86**, 2790–2793.

BATCHELOR, G. K. 1950 The application of the similarity theory of turbulence to atmospheric diffusion. *Q. J. R. Meteorol. Soc.* **76**, 133.

BEC, J. 2005 Multifractal concentrations of inertial particles in smooth random flows. *J. Fluid Mech.* **528**, 255–277.

BEC, J., BIFERALE, L., BOFFETTA, G., CELANI, A., CENCINI, M., LANOTTE, A. S., MUSACCHIO, S. & TOSCHI, F. 2006*a* Acceleration statistics of heavy particles in turbulent flows. *J. Fluid Mech.* **550**, 349–358.

BEC, J., BIFERALE, L., BOFFETTA, G., CENCINI, M., MUSACCHIO, S. & TOSCHI, F. 2006*b* Lyapunov exponents of heavy particles in turbulence. *Phys. Fluids* **18**, 091702.

BEC, J., BIFERALE, L., CENCINI, M., LANOTTE, A. S., MUSACCHIO, S. & TOSCHI, F. 2007 Heavy particle concentration in turbulence at dissipative and inertial scales. *Phys. Rev. Lett.* **98**, 084502.

BEC, J., BIFERALE, L., CENCINI, M., LANOTTE, A. S. & TOSCHI, F. 2010*b* Intermittency in the velocity distribution of heavy particles in turbulence. *J. Fluid Mech.* **646**, 527–536.

BEC, J., BIFERALE, L., CENCINI, M., LANOTTE, A. S. & TOSCHI, F. 2011 Spatial and velocity statistics of inertial particles in turbulent flows. *J. Phys.: Conf. Ser.* **333**, 012003.

BEC, J., BIFERALE, L., LANOTTE, A. S., SCAGLIARINI, A. & TOSCHI, F. 2010*a* Turbulent pair dispersion of inertial particles. *J. Fluid Mech.* **645**, 497–528.

BENNETT, A. F. 1984 Relative dispersion: local and non-local dynamics. *J. Atmos. Sci.* **41** (11), 1881–1886.

BENNETT, A. 2006 *Lagrangian Fluid Dynamics*, Cambridge Monographs on Mechanics. Cambridge University Press.

BENZI, R. 2011 *A Voyage through Turbulence* (ed. P. Davidson, Y. Kaneda, K. Moffatt & K. Sreenivasan), Cambridge University Press.

BENZI, R., BIFERALE, L., FISHER, R., LAMB, D. Q. & TOSCHI, F. 2010 Inertial range Eulerian and Lagrangian statistics from numerical simulations of isotropic turbulence. *J. Fluid Mech.* **653**, 221.

BENZI, R., CILIBERTO, S., TRIPICCIONE, R., BAUDET, C., MASSAIOLI, F. & SUCCI, S. 1993 Extended self-similarity in turbulent flows. *Phys. Rev.* E **48**, R29.

BIFERALE, L. 2008 A note on the fluctuation of dissipative scale in turbulence. *Phys. Fluids* **20**, 031703.

BIFERALE, L., BOFFETTA, G., CELANI, A., DEVENISH, B. J., LANOTTE, A. & TOSCHI, F. 2004 Multifractal statistics of Lagrangian velocity and acceleration in turbulence. *Phys. Rev. Lett.* **93**, 064502-1–064502-4.

BIFERALE, L., BOFFETTA, G., CELANI, A., DEVENISH, B. J., LANOTTE, A. & TOSCHI, F. 2005*a* Lagrangian statistics of particle pairs in homogeneous isotropic turbulence. *Phys. Fluids* **17**, 115101.

BIFERALE, L., BOFFETTA, G., CELANI, A., DEVENISH, B. J., LANOTTE, A. & TOSCHI, F. 2005*b* Multi-particle dispersion in fully developed turbulence. *Phys. Fluids* **17**, 111701.

BIFERALE, L., CALZAVARINI, E. & TOSCHI, F. 2011 Multi-time multi-scale correlation functions in hydrodynamic turbulence. *Phys. Fluids* **23**, 085107.

BIFERALE, L., LANOTTE, A. S. & TOSCHI, F. 2008 Statistical behaviour of isotropic and anisotropic fluctuations in homogeneous turbulence. *Physica* D **237**, 1969–1975.

BITANE, R., HOMANN, H. & BEC, J. 2012*a* Time scales of turbulent relative dispersion. *Phys. Rev.* E **86**, 045302(R).

BITANE, R., HOMANN, H. & BEC, J. 2012*b* Geometry and violent events in turbulent pair dispersion. *J. Turbul.* **14**, 23–45.

BOFFETTA, G. & CELANI, A. 2000 Pair dispersion in turbulence. *Physica* A **280**, 1–9.

BOFFETTA, G., CELANI, A., CRISANTI, A. & VULPIANI, A. 1999 Pair dispersion in synthetic fully developed turbulence. *Phys. Rev.* E **60**, 6734–6741.

BOFFETTA, G., DE LILLO, F. & GAMBA, A. 2004 Large scale inhomogeneity of inertial particles in turbulent flows. *Phys. Fluids* **16**, L20–L24.

BOFFETTA, G. & SOKOLOV, I. M. 2002*a* Statistics of two-particle dispersion in two-dimensional turbulence. *Phys. Fluids* **14**, 3224.

BOFFETTA, G. & SOKOLOV, I. M. 2002*b* Relative dispersion in fully developed turbulence: the Richardson's law and intermittency corrections. *Phys. Rev. Lett.* **88**, 094501.

BORGAS, M. S. 1993 The multifractal Lagrangian nature of turbulence. *Phil. Trans. R. Soc. Lond.* A **342**, 379–411.

BORGAS, M. S. & SAWFORD, B. L. 1994 A family of stochastic models for two-particle dispersion in isotropic homogeneous stationary turbulence. *J. Fluid Mech.* **279**, 69–99.

BORGAS, M. S. & YEUNG, P. K. 2004 Relative dispersion in isotropic turbulence. Part 2. A new stochastic model with Reynolds-number dependence. *J. Fluid Mech.* **503**, 125–160.

BOURGOIN, M., OUELLETTE, N. T., XU, H., BERG, J. & BODENSCHATZ, E. 2006 The role of pair dispersion in turbulent flow. *Science* **311**, 835.

CHAVES, M., GAWĘDZKI, K., HORVAI, P., KUPIAINEN, A. & VERGASSOLA, M. 2003 Lagrangian dispersion in Gaussian self-similar velocity ensembles. *J. Stat. Phys.* **113**, 643–692.

CHEN, S., DOOLEN, G. D., KRAICHNAN, R. H. & SHE, Z.-S. 1993 On statistical correlations between velocity increments and locally averaged dissipation in homogeneous turbulence. *Phys. Fluids* A **5**, 458.

CHERTKOV, M., PUMIR, A. & SHRAIMAN, B. I. 1999 Lagrangian tetrad dynamics and the phenomenology of turbulence. *Phys. Fluids* **11**, 2394.

CHUN, J., KOCH, D. L., RANI, S., AHLUWALIA, A. & COLLINS, L. R. 2005 Clustering of aerosol particles in isotropic turbulence. *J. Fluid Mech.* **536**, 219–251.

CSANADY, G. T. 1973 *Turbulent Diffusion in the Environment*. Ed. D. Reidel Publishing Company.

DIMOTAKIS, P. E. 2005 Turbulent mixing. *Annu. Rev. Fluid Mech.* **37**, 329–356.

EYINK, G. 2013 Diffusion approximation in turbulent two-particle dispersion. *Phys. Rev.* E **88**, 041001(R).

FALKOVICH, G., FOUXON, A. & STEPANOV, G. 2002 Acceleration of rain initiation by cloud turbulence. *Nature* **419**, 151.

FALKOVICH, G. & FRISHMAN, A. 2013 Single flow snapshot reveals the future and the past of pairs of particles in turbulence. *Phys. Rev. Lett.* **110**, 214502.

FALKOVICH, G., GAWĘDZKI, K. & VERGASSOLA, M. 2001 Particles and fields in fluid turbulence. *Rev. Mod. Phys.* **73**, 913–975.

FOUXON, I. & HORVAI, P. 2008 Separation of heavy particles in turbulence. *Phys. Rev. Lett.* **100**, 04061.

FRISCH, U. 1995 *Turbulence. The Legacy of A. N. Kolmogorov*. Cambridge University Press.

FUNG, J. C. H. & VASSILICOS, J. C. 1998 Two-particle dispersion in turbulent-like flows. *Phys. Rev.* E **57**, 1677.

ILYIN, V., PROCACCIA, I. & ZAGORODNY, A. 2013 Fokker–Planck equation with memory: the crossover from ballistic to diffusive processes in many-particle systems and incompressible media. *Cond. Matter Phys.* **16** (1), 13004: 1–18.

JENSEN, M.-H. 1999 Multiscaling and structure functions in turbulence: an alternative approach. *Phys. Rev. Lett.* **83**, 76.

JULLIEN, M.-C. 2003 Dispersion of passive tracers in the direct enstrophy cascade: experimental observations. *Phys. Fluids* **15**, 2228–2237.

JULLIEN, M.-C., PARET, J. & TABELING, P. 1999 Richardson pair dispersion in two-dimensional turbulence. *Phys. Rev. Lett.* **82**, 2872.

KANATANI, K., OGASAWARA, T. & TOH, S. 2009 Telegraph-type versus diffusion-type models of turbulent relative dispersion. *J. Phys. Soc. Japan* **78**, 024401.

KLAFTER, J., BLUMEN, A. & SHLESINGER, M. F. 1987 Stochastic pathway to anomalous diffusion. *Phys. Rev.* A **35**, 3081–3085.

KRAICHNAN, R. H. 1966 Dispersion of particle pairs in homogeneous turbulence. *Phys. Fluids* **9**, 1937–1943.

KURBANMURADOV, O. A. 1997 Stochastic Lagrangian models for two-particle relative dispersion in high-Reynolds number turbulence. *Monte Carlo Meth. Applic.* **3**, 37–52.

LACASCE, J. H. 2010 Relative displacement probability distribution functions from balloons and drifters. *J. Mar. Res.* **68**, 433–457.

LACORATA, G., MAZZINO, A. & RIZZA, U. 2008 3D chaotic model for subgrid turbulent dispersion in large eddy simulations. *J. Atmos. Sci.* **65**, 2389–2401.

LEPRETI, F., CARBONE, V., ABRAMENKO, V. I., YURCHYSHYN, V., GOODE, P. R., CAPPARELLI, V. & VECCHIO, A. 2012 Turbulent pair dispersion of photospheric bright points. *Astrophys. J. Lett.* **759**, L17.

LUNDGREN, T. S. 1981 Turbulent pair dispersion and scalar diffusion. *J. Fluid Mech.* **111**, 27–57.

MALIK, N. A. & VASSILICOS, J. C. 1999 A Lagrangian model for turbulent dispersion with turbulent-like flow structure: comparison with direct numerical simulation for two-particle statistics. *Phys. Fluids* **11**, 1572.

MASOLIVER, J. & WEISS, G. H. 1996 Finite-velocity diffusion. *Eur. J. Phys.* **17**, 190–196.

MAZZITELLI, I. M., FORNARELLI, F., LANOTTE, A. S. & ORESTA, P. 2014 Pair and multi-particle dispersion in numerical simulations of convective boundary layer turbulence. *Phys. Fluids* **26**, 055110.

MONIN, A. S. & YAGLOM, A. M. 1975 *Statistical Fluid Mechanics*. MIT Press, c1971-1975.

MORDANT, N., METZ, P., MICHEL, O. & PINTON, J.-F. 2001 Measurement of Lagrangian velocity in fully developed turbulence. *Phys. Rev. Lett.* **87**, 214501.

NI, R. & XIA, K.-Q. 2013 Experimental investigation of pair dispersion with small initial separation in convective turbulence. *Phys. Rev.* E **87**, 063006.

NICOLLEAU, F. C. G. A. & NOWAKOWSKI, A. F. 2011 Presence of a Richardson's regime in kinematic simulations. *Phys. Rev.* E **83**, 056317.

NOVIKOV, E. A. 1989 Two-particle description of turbulence, Markov property and intermittency. *Phys. Fluids* A **1** (2), 326–330.

OLLITRAUT, M., GABILLET, C. & COLIN DE VERDIÉRE, A. 2005 Open ocean regimes of relative dispersion. *J. Fluid Mech.* **533**, 381–407.

OTT, S. & MANN, J. 2000 An experimental investigation of the relative diffusion of particle pairs in three-dimensional turbulent flow. *J. Fluid Mech.* **422**, 207–223.

PAGNINI, G. 2008 Lagrangian stochastic models for turbulent relative dispersion based on particle pair rotation. *J. Fluid Mech.* **616**, 357–395.

PAN, L. & PADOAN, P. 2010 Relative velocity of inertial particles in turbulent flows. *J. Fluid Mech.* **661**, 73–107.

POULAIN, P. M. & ZAMBIANCHI, E. 2007 Surface circulation in the central Mediterranean Sea as deduced from Lagrangian drifters in the 1990s. *Cont. Shelf Res.* **27**, 981–1001.

RICHARDSON, L. F. 1926 Atmospheric diffusion shown on a distance-neighbour graph. *Proc. R. Soc. Lond.* A **110**, 709.

SALAZAR, J. P. L. C. & COLLINS, L. R. 2009 Two-particle dispersion in isotropic turbulent flows. *Annu. Rev. Fluid Mech.* **41**, 405–432.

SALAZAR, J. P. L. C. & COLLINS, L. R. 2012 Inertial particle relative velocity statistics in homogeneous isotropic turbulence. *J. Fluid Mech.* **696**, 45–66.

SAWFORD, B. 2001 Turbulent relative dispersion. *Annu. Rev. Fluid Mech.* **33**, 289–317.

SAWFORD, B. L., YEUNG, P. K. & BORGAS, M. S. 2005 Comparison of backwards and forwards relative dispersion in turbulence. *Phys. Fluids* **17**, 095109.

SCATAMACCHIA, R., BIFERALE, L. & TOSCHI, F. 2012 Extreme events in the dispersions of two neighboring particles under the influence of fluid turbulence. *Phys. Rev. Lett.* **109**, 144501.

SCHUMACHER, J. 2007 Sub-Kolmogorov-scale fluctuations in fluid turbulence. *Europhys. Lett.* **80**, 54001.

SCHUMACHER, J. 2008 Lagrangian dispersion and heat transport in convective turbulence. *Phys. Rev. Lett.* **100**, 134502.

SOKOLOV, I. M. 1999 Two-particle dispersion by correlated random velocity fields. *Phys. Rev.* E **60**, 5528.

SREENIVASAN, K. R. & ANTONIA, R. A. 1997 The phenomenology of small-scale turbulence. *Annu. Rev. Fluid Mech.* **29**, 435–472.

THALABARD, S., KRSTULOVIC, G. & BEC, J. 2014 Turbulent pair dispersion as a continuous-time random walk, http://arxiv.org/abs/1405.7315.

THOMSON, D. J. 1990 A stochastic model for the motion of particle pairs in isotropic high-Reynolds-number turbulence, and its application to the problem of concentration variance. *J. Fluid Mech.* **210**, 113–153.

THOMSON, D. J. & DEVENISH, B. J. 2005 Particle pair separation in kinematic simulations. *J. Fluid Mech.* **526**, 277.

WILKINSON, M. & MEHLIG, B. 2005 Caustics in turbulent aerosols. *Europhys. Lett.* **71**, 186–192.

XU, H., BOURGOIN, M., OUELLETTE, N. T. & BODENSCHATZ, E. 2006 High order Lagrangian velocity statistics in turbulence. *Phys. Rev. Lett.* **96**, 024503.

XU, H., PUMIR, A. & BODENSCHATZ, E. 2011 The pirouette effect in turbulence. *Nat. Phys.* **7**, 709–712.

YAKHOT, V. 2006 Probability densities in strong turbulence. *Physica* D **215**, 166.